HEFAT2010
7th International Conference on Heat Transfer, Fluid Mechanics and Thermodynamics
19-21 July 2010
Antalya, Turkey

DESIGNED MICRO-CHANNEL HEAT SINKS USING MATHEMATICAL OPTIMIZATION WITH VARIABLE AXIAL LENGTH

Ighalo F.U., Bello-Ochende T*., Meyer J.P.
*Author for correspondence
Department of Mechanical and Aeronautical Engineering,
University of Pretoria,
Pretoria, 0002,
South Africa,
E-mail: tbochende@up.ac.za

ABSTRACT

This paper documents the geometrical optimization of a micro-channel heat sink with a relaxed axial length. The objective is to optimize (minimize) the wall peak temperature of the heat sink subject to various constraints such as manufacturing restraints, fixed pressure drop and total fixed volume. A gradient based optimization algorithm is used as it adequately handles the numerical objective function obtained from computational fluid dynamics simulation. Optimal geometric parameters defining the micro-channel were obtained for a pressure drop ranging from 10 kPa to 60 kPa corresponding to dimensionless pressure drop of $6.5x10^7$ to $4x10^8$. The effect of pressure drop on the aspect ratio, solid volume fraction, channel hydraulic diameter and the minimized peak temperature are reported. Results also show that as the pressure drop increases the maximum global thermal conductance also increases. These results are in agreement with previous work found in literature.

INTRODUCTION

The impact of the new generation drive for high processing speed of sophisticated and compact electronic devices is the rising transistor density and switching speed of microprocessors. This challenge results in an increase in the amount of heat flux dissipation which is predicted to be in the excess of 100 W/cm^2 in the near future [1,2]. With this comes the need for advanced cooling techniques and micro-channels have recently generated great interest by researchers as it proves to yield high heat transfer rates.

Tuckerman and Pease [3] in 1981 proposed that single phased microscopic heat exchangers using water as the coolant could achieve power density cooling of up to 1000 W/cm^2 and with experimentation; the cooling water could dissipate a heat flux of about 790 W/cm^2. Dirker and Meyer [4] developed correlations that predict the cooling performance of heat spreading layers in rectangular heat generating electronic modules. They discovered that the thermal performance was dependent on the geometric size of the volume posed by the presence of thermal resistance. However, shape and various geometrical parameters such as the aspect ratio of a micro-channel have a great influence on the heat transfer capabilities of these heat sinks [5]. Wu and Cheng [6] experimentally showed that though the hydraulic diameter of various micro-channels may be the same, their friction factor may differ if their geometrical shapes are different. Also, the friction factor increases as the aspect ratio of the micro-channel is increased. Most recently, Bello-Ochende *et al.* [7] and Muzychka [8] used the constructal design theory and intersection of asymptotes method to determine optimal geometric configurations that maximize the global thermal conductance in a dimensionless form.

In this work, an optimal geometry for a micro-channel heat sink is numerically determined which minimizes the peak wall temperature using mathematical optimization.

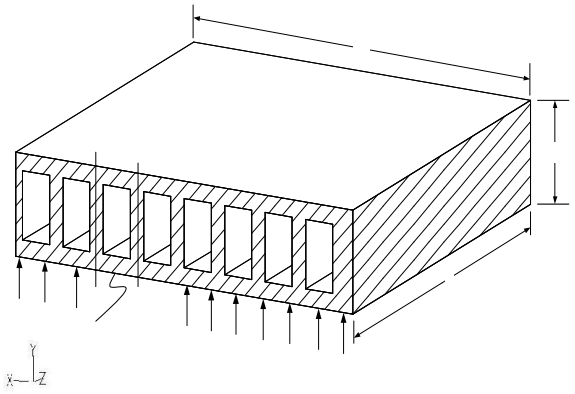

Figure 1 Physical model of a micro-channel heat sink

NOMENCLATURE

A	[m^2]	Channel cross-sectional area
B	[m]	Channel width
Be	[-]	Bejan number
C	[-]	Global thermal conductance
C_p	[J/Kg]	Specific heat capacity
D	[m]	Diameter
$f(x)$	[-]	Objective function
$g_i(x)$	[-]	i-th equality constraint function
G	[m]	Computational domain width
$h_j(x)$	[m]	j-th equality constraint function
H	[m]	Computational domain height
k	[W/m.K]	Thermal conductivity
L	[m]	Channel axial length
P	[Pa]	Pressure
$P[k]$	[-]	Successive sub-problem
q''	[W/m^2]	Heat flux
$\mathbb{R}^n$	[-]	n-dimensional real space
T	[K]	Temperature
t_1	[m]	Half thickness of vertical solid
t_2	[m]	Channel base thickness
t_3	[m]	Channel base to height distance
U	[m/s]	Velocity
V	[m^3]	Volume
W	[m]	Heat sink width
x,y,z	[-]	Cartesian coordinates

Special characters

α	[m^2/s]	Thermal diffusivity
Δ	[-]	Difference
μ	[kg/m.s]	Dynamic viscosity
ρ	[kg/m^3]	Density
ϕ	[-]	Solid volume fraction
∂	[-]	Step limit

Subscripts

c	Channel
f	Fluid
h	Hydraulic
max	Maximum
min	Minimum
opt	Optimum
s	Solid

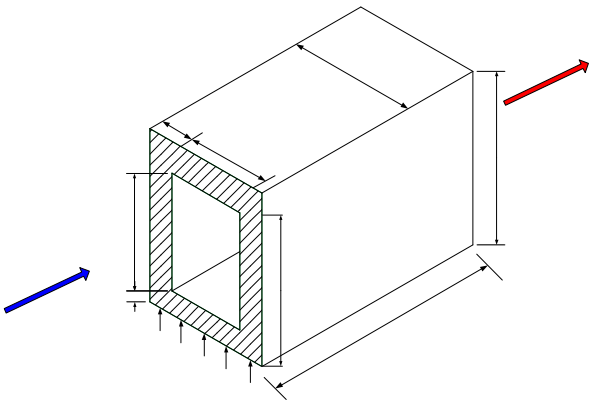

Figure 2 Modelling computational domain

COMPUTATIONAL MODEL

Figure 1 shows the physical model and Figure 2 the computational domain for a micro-channel heat sink. The computational domain is an elemental volume selected from a complete micro-channel heat sink by the use of the symmetrical property of the heat sink. Heat is supplied to a highly conductive silicon substrate with known thermal conductivity from a heating area located at the bottom of the heat sink. The heat is then removed by a fluid flowing through a number of micro-channels.

The following assumptions were made to model the heat transfer and fluid flow in the elemental volume: the hydraulic diameter of the micro-channel under analysis is greater than 10 μm. For water, the continuum regime applies hence the Navier-Stokes and Fourier equations can still be used to describe the transport processes; steady-state conditions for flow and heat transfer; incompressible flow; the properties of the solid and fluid are constant; and the heat transfer due to radiation and natural convection is negligible. It is also assumed that the number of elemental micro-channels is large.

Based on the assumptions listed above, the continuity, momentum and energy equations governing the fluid flow and heat transfer for the cooling fluid within the heat sink are given in equations (1), (2) and (3) respectively.

$$\nabla(\rho \boldsymbol{U}) = 0 \tag{1}$$

$$\rho(\boldsymbol{U}.\nabla \boldsymbol{U}) + \Delta P - \mu \nabla^2 \boldsymbol{U} = 0 \tag{2}$$

$$\rho C_p(\boldsymbol{U}.\nabla T) - k_f \nabla^2 T = 0 \tag{3}$$

For the solid material, the momentum and energy governing equations are given by equation (4) below.

$$\boldsymbol{U} = 0, \qquad k_s \nabla^2 T \tag{4}$$

The conjugate heat transfer problem is modelled with heat being supplied to the bottom wall of the heat sink at 1 MW/m^2 with water at 20°C pumped across the channel length. A vertex-centred finite volume code was used to solve the continuity, momentum and energy equations using the appropriate boundary conditions. A second order upwind scheme was used in discretizing the momentum equation while a SIMPLE algorithm was used for the pressure-velocity coupling. Convergence criteria was set to less than $1x10^{-4}$ for continuity and momentum residuals while the residual of energy was set to less than $1x10^{-7}$. To ensure accuracy of the results, mesh refinement was performed until a mesh size with negligible changes in thermal resistance was obtained.

NUMERICAL OPTIMIZATION

A robust gradient based optimization algorithm which does not require an explicit line search is used for the mathematical optimization of the conjugate heat transfer problem. The DYNAMIC-Q optimization algorithm applies the dynamic trajectory LFOPC optimization algorithm to successive quadratic approximations of the actual optimization problem [9]. Consider a typical constrained optimization problem of the form:

$$\underset{\text{with respect to x}}{\text{minimize}}\ \mathrm{f}(\boldsymbol{x}),\ \ \boldsymbol{x}=[x_1,x_2,..x_l..,x_n]^T, x_l\in\mathbb{R}^n$$
subject to the constraints:
$$\mathrm{g}_i(\boldsymbol{x})\le 0,\ \ i=1,2,...,m \qquad (5)$$
$$\mathrm{h}_j(\boldsymbol{x})=0,\ \ j=1,2,...,r$$

In this method, successive sub-problems $P[k],\ k=0,1,2,...$ are generated at successive design points $\boldsymbol{x}^k$ by constructing spherically quadratic approximations which are used to approximate the objective functions or constraints (or both) if they are not analytically given or very expensive to compute numerically [10, 11]. These spherical quadratic approximations are given by:

$$\tilde{\mathrm{f}}(\boldsymbol{x})=\mathrm{f}(\boldsymbol{x}^k)+\nabla^T\mathrm{f}(\boldsymbol{x}^k)(\boldsymbol{x}-\boldsymbol{x}^k)+\frac{1}{2}(\boldsymbol{x}-\boldsymbol{x}^k)\mathbf{A}(\boldsymbol{x}-\boldsymbol{x}^k)$$
$$\tilde{\mathrm{g}}_i(\boldsymbol{x})=\mathrm{g}_i(\boldsymbol{x}^k)+\nabla^T\mathrm{g}_i(\boldsymbol{x}^k)(\boldsymbol{x}-\boldsymbol{x}^k)+\frac{1}{2}(\boldsymbol{x}-\boldsymbol{x}^k)\mathbf{B}_i(\boldsymbol{x}-\boldsymbol{x}^k) \qquad (6)$$
$$\tilde{\mathrm{h}}_j(\boldsymbol{x})=\mathrm{h}_j(\boldsymbol{x}^k)+\nabla^T\mathrm{h}_j(\boldsymbol{x}^k)(\boldsymbol{x}-\boldsymbol{x}^k)+\frac{1}{2}(\boldsymbol{x}-\boldsymbol{x}^k)\mathbf{C}_j(\boldsymbol{x}-\boldsymbol{x}^k)$$

$\boldsymbol{A}$, $\boldsymbol{B}_i$ and $\boldsymbol{C}_j$ being Hessian matrices of the objective, inequality and equality functions respectively. The gradient vector is approximated by means of a forward finite difference scheme as the objective function is obtained numerically from a CFD simulation. The finite differencing scheme used is as follows:

$$\frac{\partial \mathrm{f}(\boldsymbol{x})}{\partial x_l}=\frac{\mathrm{f}(\boldsymbol{x}+\Delta\boldsymbol{x}_l)-\mathrm{f}(\boldsymbol{x})}{\Delta\boldsymbol{x}_l}\ \ \forall\ l=1,2,...,n \qquad (7)$$

with $\Delta\boldsymbol{x}_l=[0,0,...,\Delta x_l,...0]^T$ being an appropriate differencing step size. The constraints gradient vectors on the other hand are provided analytically.

In order to achieve convergence in a stable and controlled form, move limits are used in the DYNAMIC-Q algorithm. The move limit takes on the form of a constraint by limiting the movement of each design variables by not allowing the new design point to move too far away from the current design point. This additional constraint is of the form:

$$\boldsymbol{x}_l-\boldsymbol{x}_l^k-\boldsymbol{\delta}_l\le 0$$
$$-\boldsymbol{x}_l+\boldsymbol{x}_l^k-\boldsymbol{\delta}_l\le 0 \qquad (8)$$
$$\text{with } l=1,2,...,n$$

The DYNAMIC-Q algorithm terminates when the norm of the step size or function value is less than a specified tolerance.

OPTIMIZATION PROBLEM

The optimization problem aims to find the best micro-channel heat sink geometric parameters that give the minimum peak temperature for a fixed pressure drop and total volume. This optimal value is achieved by the relaxation of the geometric parameters t_1, t_2, t_3, *H and G* for the fixed axial length case and an additional variable *L* as depicted in Figure 2 for the variable length case.

Constraints

- Solid Volume Fraction: The solid volume fraction ϕ which is defined as the ratio of solid volume material to the total volume of the micro-channel heat sink is allowed to vary between 0.3 and 0.8.

$$0.3\le\left[\phi=\frac{V_s}{V}=\frac{A_sL}{AL}=\frac{A_s}{A}\right]\le 0.8 \qquad (9)$$

- Manufacturing Restraints: Assuming the DRIE manufacturing technique [12, 13] was employed in the fabrication of the heat sink, the maximum allowable aspect ratio is 20. Also the minimum allowable thickness of the top and bottom wall is 50 μm [14, 15].
- Total Fixed Volume: For each optimization problem, the computational volume is kept constant.

Optimization Procedure

The optimization problem presented in previous section was solved by coupling The DYNAMIC-Q optimization algorithm with computational fluid dynamics (FLUENT [16]) and grid generation (GAMBIT [17]) code in a MATLAB [18] environment. Figure 3 gives a flow guide to how the automation is carried out until convergence (either by step size or function value criteria) is reached. To ensure that the converged solution obtained is indeed the global minimum, a multi starting guess approach is used.

Figure 3 Optimization process flow chart

TRENDS AND RESULTS

The optimization problem formulated above is now applied to a given computational volume V = 0.9 mm^3 with a fixed pressure drop varying from 10 kPa to 60 kPa. The five design geometric parameters are then varied to determine the minimum peak temperature and the effect of pressure drop on the solid volume fraction, hydraulic diameter, channel aspect ratio and other heat transfer parameters.

Figure 4 shows the effects of the minimised wall peak temperature difference ΔT_{min} of the micro-channel with respect to the change in the applied fixed pressure drop. It shows a non-linear decrease in ΔT_{min} because of the increased forced convection heat transfer made possible with the increase in the applied pressure drop across the micro-channel length. The trend is in agreement with already published work in the open literature [7,14,19]. This shows that drastic cooling capabilities can be achieved by using adequate pumping power; however a trade-off will always be required.

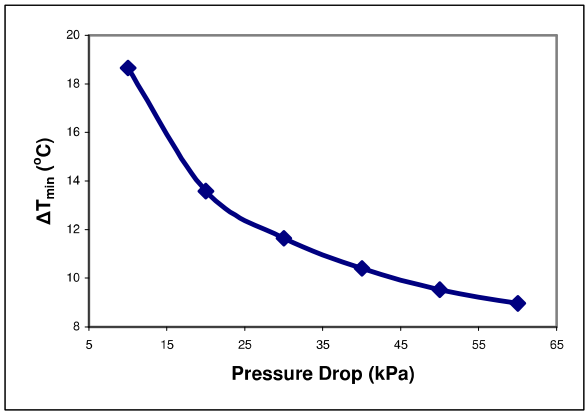

Figure 4 The influence of pressure drop on the optimized peak wall temperature

Figure 5 shows the effect of pressure drop on the optimal solid volume fraction ϕ_{opt}. As the pressure drop increases , ϕ_{opt} also increases. An approximate linear relationship exist between ϕ_{opt} and the pressure drop. The trend also shows that the optimal solid volume fraction ranges between 0.3 and 0.5 which agrees with the results published by Bello-Ochende *et al*. [7].

A decrease in the optimal hydraulic diameter (Figure 6) of the heat sink is also observed with an increase in the pressure drop applied across the channel. This decrease continues until it is such that the cooling fluid is been "squeezed" into the channel. Further increase in the pressure drop causes the optimal hydraulic diameter to increase in order to ensure the flow is not overworked. The optimal hydraulic diameter trend for a pressure drop range between 10 kPa and 60 kPa is shown in figure 6. The optimal hydraulic diameter ranges from 120 µm to 140 µm and this validates the assumption made when defining our computational model.

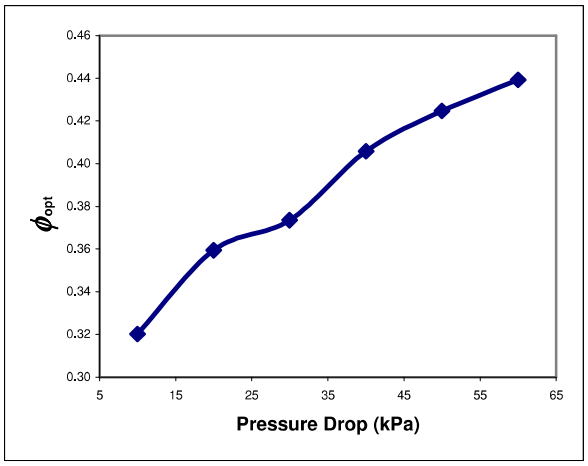

Figure 5 The influence of pressure drop on the optimal volume fraction

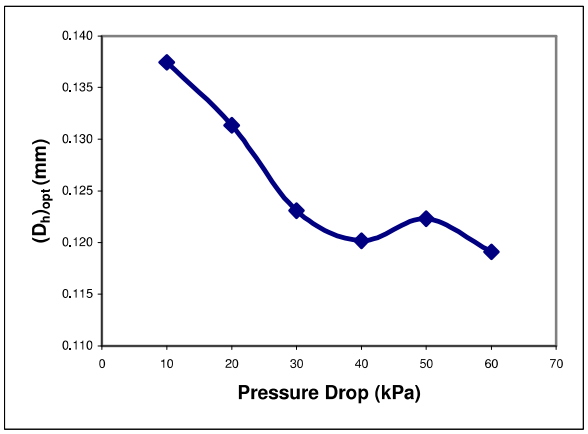

Figure 6 The effect of pressure drop on the optimal hydraulic diameter

The optimization process was then executed with the length not fixed to 10 mm but relaxed which increases the degrees of freedom of the heat sink thereby obtaining an optimal length. It proved to offer better optimal cooling effects as shown in Figure 7 at lower pressure drops with a more than 16% decrease in the optimal peak wall temperature difference at 10 kPa.

Table 1 gives the optimal design parameters for the heat sink when the axial length is relaxed. The results show a linear increasing trend of the optimized aspect ratio as a function of the applied pressure drop with the ratio of solid volume to total volume between 0.4 and 0.45. This optimal configuration provides improved heat transfer capabilities with an increased maximized global thermal conductance of the heat sink of up to 20% at low pressures as shown in Figure 8. Figure 8 also shows that the maximised dimensionless global thermal conductance increases linearly with the dimensionless pressure drop (Bejan number) which is defined as:

$$Be = \frac{\Delta P V^{2/3}}{\alpha \mu} \tag{10}$$

The maximized global thermal conductance is expressed as:

$$C_{\max} = \frac{q''L}{k(\Delta T_{\max})_{\min}} \tag{11}$$

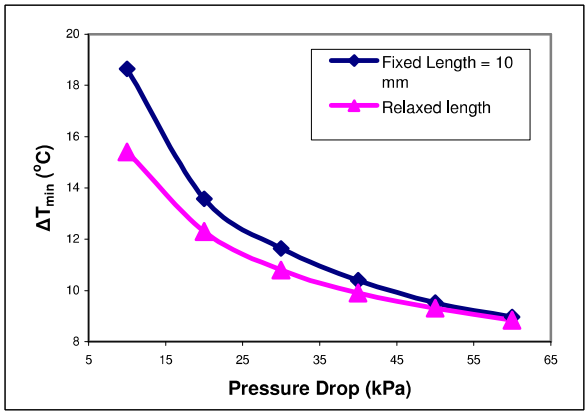

Figure 7 The effect of the relaxation of the axial length as compared to the fixed length optimal peak wall temperature

Table 1 Optimal design results with relaxed axial length

Pressure Drop (kPa)	Optimised Aspect Ratio $(H_c/B)_{opt}$	Optimised Volume Fraction ϕ_{opt}	$(D_h)_{opt}$ (mm)
60	11.831	0.440	0.126
50	11.341	0.439	0.131
40	10.753	0.440	0.139
30	10.079	0.429	0.149
20	9.170	0.407	0.161
10	7.873	0.382	0.188

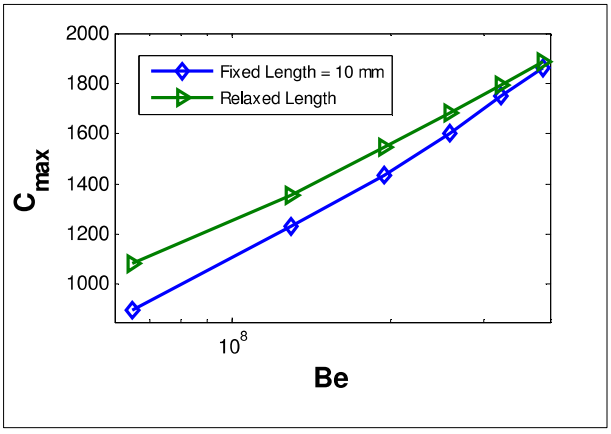

Figure 8 Heat transfer enhancement by length relaxation

Figure 9 depicts a linear relationship between the optimized length and the applied pressure drop. The result shows that as the pressure drop is increased, the resulting optimal channel configuration will be of a longer but slender nature. Figure 10 shows the optimal static temperature contour of the heat sink when a pressure difference of 50 kPa is applied along its length and transversely at the exit of the heat sink. The solution of the conjugate heat transfer problem shows a gradual increase in temperature across the channel length from the fluid inlet to its outlet with the hot spot located at the bottom wall.

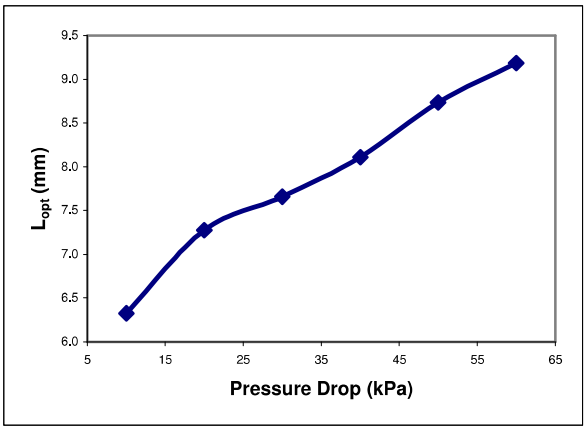

Figure 9 The optimal axial length as a function of the applied pressure drop

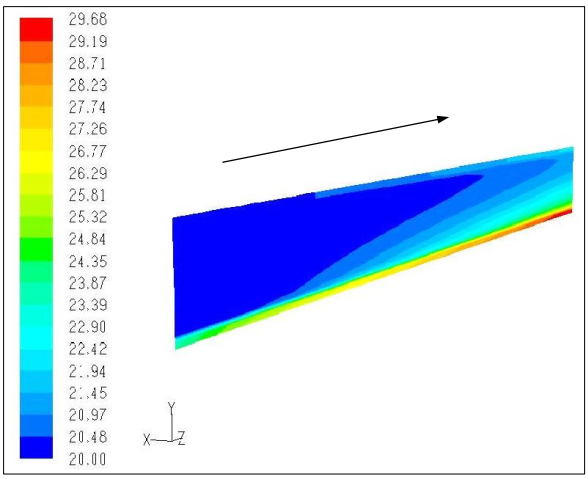

Figure 10a Temperature contours (in °C) across the length of the heat sink. It shows the gradual increase in temperature along its length.

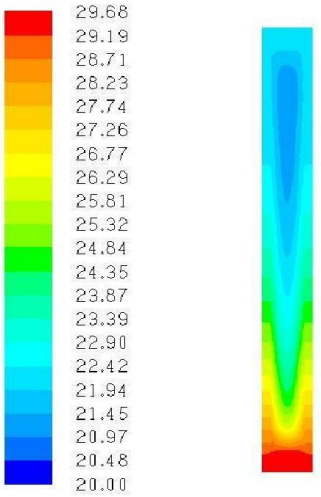

Figure 10b Temperature contours (in °C) across the transverse axis showing an increase in temperature from the channel top wall to the hot spot bottom wall.

CONCLUSION

In this paper, it has been demonstrated that numerical simulations and mathematical optimization can be used to optimally design micro-channels. For a pressure drop range between 10 kPa and 60 kPa, the optimal peak wall temperature decreased exponentially with an increase in pressure. It has been shown that a unique optimal geometric configuration exists for a given pressure drop applied across a channel that will result in a minimized peak wall temperature. Furthermore, taking more design parameters into account will result in even better cooling capabilities of micro-channel heat sinks as up to 20% increase in the global thermal conductance were obtained when the axial length was relaxed in the optimization process.

REFERENCES

[1] F.J. Hong, P. Cheng, H. Ge, Goh Teck Joo, 'Conjugate heat transfer in fractal-shaped microchannel network heat sink for integrated micoelectronic cooling application', *International Journal of Heat and Mass Transfer*, Vol. 50, pp. 4986-4998, 2007.

[2] K.C. Toh, X.Y. Chen, J.C. Chai, 'Numerical computation of fluid flow and heat transfer in microchannels', *International Journal of Heat and Mass Transfer*, Vol. 45, pp. 5133-5141, 2002.

[3] D. B. Tuckerman, R.F.W. Pease, 'High performance heat sinking for VLSI', *IEE Electron Device Letters*, EDL-2, pp. 126-129, 1981.

[4] J. Dirker, J. P. Meyer, 'Thermal characterisation of embedded heat spreading layers in rectangular heat-generating electronic modules', *International Journal of Heat and Mass Transfer*, Vol. 52, pp. 1374-1384, 2009.

[5] H.Y. Wu, Ping Cheng, 'An experimental study of convective heat transfer in silicon microchannels with different surface conditions', *International Journal of Heat and Mass Transfer*, Vol. 46, pp. 2547–2556, 2003.

[6] H.Y. Wu, Ping Cheng, 'Friction factors in smooth trapezoidal silicon microchannels with different aspect ratios', *International Journal of Heat and Mass Transfer*, Vol. 46, pp. 2519–2525, 2003.

[7] T. Bello-Ochende, L. Liebenberg, J.P. Meyer, 'Constructal cooling channels for micro-channel heat sinks', *International Journal of Heat and Mass Transfer*, Vol. 50, pp. 4141-4150, 2007.

[8] Y. S. Muzychka, 'Constructal design of forced convection cooled microchannel heat sinks and heat exchangers', *International Journal of Heat and Mass Transfer,* Vol. 48, pp. 3119–3127, 2005.

[9] J.A. Snyman, *Practical Mathematical Optimization: An Introduction to Basic Optimization Theory and Classical and New Gradient-Based Algorithms,* Springer, New York, 2005.

[10] J.A. Snyman, A.M. Hay, 'The DYNAMIC-Q Optimization Method: An Alternative to SQP?', *Computer and Mathematics with Applications*, Vol. 44, pp. 1589-1598, 2002.

[11] De Kock, D. J., Optimal Tundish Methodology in a Continuous Casting Process. PhD Thesis, Department of Mechanical and Aeronautical Engineering, University of Pretoria, 2005.

[12] F. Laermer, A. Urban, 'Challenges, developments and application of silicon deep reactive ion etching', *Microelectronic Engineering,* Vol. 67-68, pp. 349-355, 2003.

[13] M. J. Madou, "MEMS Fabrication," in *MEMS Handbook,* M. Gad-el-Hak, Ed., Boca Raton, FL: CRC, 2002.

[14] Afzal Husain, Kwang-Yong Kim, 'Shape Optimization of Micro-Channel Heat Sink for Micro-Electronic Cooling', *IEEE Transactions on Components and Packaging Technologies,* Vol. 31, No. 2, pp. 322-330, 2008.

[15] Ji Li, G. P. Peterson, 'Geometric Optimization of a Micro Heat Sink with Liquid Flow', *IEEE Transactions on Components and Packaging Technologies,* Vol. 29, No. 1, pp. 145-154, 2006.

[16] Fluent Inc., *Fluent Version 6 Manuals*, Centerra Resource Park, 10 Cavendish Court, Lebanon, New Hampshire, USA, 2001 (www.fluent.com).

[17] Fluent Inc., *Gambit Version 6 Manuals*, Centerra Resource Park, 10 Cavendish Court, Lebanon, New Hampshire, USA, 2001 (www.fluent.com).

[18] The MathWorks, Inc., *MATLAB & Simulink Release Notes for R2008a,* 3 Apple Hill Drive, Natick, MA, 2008 (www.mathworks.com).

[19] Afzal Husain, Kwang-Yong Kim, 'Multiobjective Optimization of a Microchannel Heat Sink using Evolutionary Algorithm', *Journal of Heat Transfer,* Vol. 130, pp. 1-3, 2008.